Metallogr. Microstruct. Anal. (2013) 2:234–241
DOI 10.1007/s13632-013-0079-3

TECHNICAL ARTICLE

# Effect of Heat Treatment on Microstructure and Mechanical Properties of 12Cr–10Ni–0.25Ti–0.7Mo Stainless Steel

**S. Chenna Krishna · J. Srinath · Abhay K. Jha · Bhanu Pant · S. C. Sharma · Koshy M. George**

Received: 27 March 2013 / Revised: 16 May 2013 / Accepted: 21 May 2013 / Published online: 19 June 2013


**Abstract** In this investigation, a precipitation hardenable martensitic stainless steel (12Cr–10Ni–0.25Ti–0.7Mo) was subjected to different heat treatment cycles to study their influence on the microstructure and mechanical properties. The heat treatment cycles include solution treatment (S), cryogenic treatment (C), and aging (A). Two solution treatment temperatures, 750 and 1000 °C, and two aging temperatures, 250 and 500 °C, were selected. Solution treatment was followed by a cryogenic treatment at −70 °C for 2 h and an aging treatment at the aforementioned temperatures. Transmission electron microscopy of the solution-treated samples showed four phases: martensite matrix, $M_{23}C_6$ carbide, Ti(C, N), and retained austenite. On aging at 500 °C, an additional phase ($Ni_3Ti$ precipitates) was observed in the martensite matrix. Mechanical properties were evaluated at room temperature for all the heat-treated samples. A reasonable increase in yield strength (YS) was observed after cryogenic treatment possibly due to transformation of retained austenite to martensite. After aging at 500 °C, a significant increase in the YS was observed over solution-treated condition. This increase in YS after aging is attributed to precipitation of fine $Ni_3Ti$ precipitates. Solution treatment temperature had an insignificant effect on the mechanical properties of the stainless steel.

S. Chenna Krishna (✉) · J. Srinath · A. K. Jha · B. Pant · S. C. Sharma
Materials and Metallurgy Group, Materials and Mechanical Entity, Vikram Sarabhai Space Centre, Trivandrum 695 022, India
e-mail: chenna.sk@gmail.com

K. M. George
Materials and Mechanical Entity, Vikram Sarabhai Space Centre, Trivandrum 695 022, India

**Keywords** Cryogenic treatment · Aging · Mechanical properties · Martensitic stainless steel

## Introduction

Precipitation hardenable (PH) stainless steels are widely used in the aerospace industry due to their high strength, weldability, good toughness, and adequate ductility. These steels are most commonly strengthened by the formation of fine intermetallics consisting of Ni, Ti, Al, and Mo [1–4]. However, a few PH steels gain strength by the precipitation of a copper-rich phase, with copper as the major precipitating element. 17-4 PH stainless steel is one such high strength steel strengthened by copper precipitates [5–7]. The steel used in this study is 12Cr–10Ni martensitic stainless steel with minor additions of molybdenum and titanium. Molybdenum is added to improve the resistance to tempering [8]. Titanium plays a key role as a strengthening element by formation of $Ni_3Ti$ precipitates during aging treatment [1–4]. In addition to increasing strength, titanium also fixes the carbon and nitrogen by forming fine Ti(C, N) [9–11]. This steel has an austenitic structure above 700 °C which transforms to martensite on air cooling [12]. Hence, solution treatment is performed at temperatures above 750 °C and preferably around 1000 °C to dissolve the carbides and other particles to attain a homogenous austenite structure. A small amount of retained austenite forms after the solution treatment along with martensite. Retained austenite is not desirable in most cases as it prevents the steel from attaining its maximum strength and induces instability in the materials performance due to the possibility of transformation during the service. Cryogenic treatment is widely employed for such steels to ensure that martensitic transformation is complete [13, 14]. It was reported that the cryogenic treatment would

also promote secondary carbide precipitation and provide other advantages, such as higher strength, increased wear resistance, and improved dimensional and microstructural stability, depending on the composition of the steel [15, 16]. The literature available on the effect of heat treatments on the mechanical properties of the current steel is limited. Therefore, an attempt was made to study the same with an aim to design the heat treatment to obtain the optimum properties.

## Experimental

The material used in this study was produced through vacuum induction melting (VIM) and refined by vacuum arc remelting (VAR). The chemical composition of the steel is given in Table 1. The cast ingot was converted to bars by forging in the temperature range of 1000–1080 °C. These bars were hot rolled to realize a plate of 4 mm thick. Samples from this plate were subjected to different heat treatment cycles. They were solution-treated at two temperatures, 750 and 1000 °C, for 0.5 h and were subsequently air cooled. These solution-treated samples were subjected to the cryogenic treatment at −70 °C for 2 h, after which they were left in air to return to room temperature. After the cryogenic treatment, the samples were aged at two different temperatures, 250 and 500 °C, with a holding time of 2 h, followed by air cooling. The heat treatment cycles employed in the study will be designated hereafter as 10S, 7S, 10SC, 7SC, 10SCA, 10SCLA, 7SCA, and 7SCLA, the details of which are given in Table 2. The heat-treated specimens were characterized for microstructure and mechanical properties.

Light microscopy of the samples was performed by conventional polishing techniques using different grades of emery papers, alumina paste, and diamond paste. The polished samples were etched with 10 mL $HNO_3$ + 10 mL acetic acid + 15 mL HCl + 2–5 drops glycerin. Hardness measurements were made with a Rockwell hardness tester using a major load of 150 kg. An average of six readings was taken for reporting the hardness for a particular heat-treated condition. Tensile properties of the steel were evaluated at room temperature as per ASTM E8M. All the specimens for tensile testing were fabricated after the heat treatment. Tests were conducted at a strain rate of $10^{-3}$ $s^{-1}$ using a universal testing machine.

Thin foils for TEM were prepared by cutting 300-μm-thick slices from the samples using a low speed saw; slices were further reduced to about 100 μm by polishing both sides of the foil using SiC emery paper. Disks of 3 mm diameter were punched from these thin foils. One side of the 3 mm disk was dimpled, followed by ion milling with an incident beam angle of 4°. The thin foils were examined with a transmission electron microscope (TEM) equipped with energy dispersive x-ray spectroscopy (EDS) operated at 200 kV.

## Results and Discussion

### Microstructure

The microstructure of the solution-treated steel at 750 and 1000 °C consists of martensite and retained austenite with some carbides, as shown in Fig. 1. The carbon content in the present steel was very low (0.018 wt%), so the martensite observed was lath martensite. The typical microstructure of 7S and 10S samples is shown in Fig. 1(a and b), respectively. The martensite laths were fine in the case of 7S samples, and the width of laths increased with increase in temperature. It was suggested in the literature that austenite grains coarsen in the temperature range of 1000–1050 °C [8, 10, 13, 14]. Strong carbide formers, such as Cr, Ti, and Nb, inhibit the austenite grain growth below 1000 °C by pinning the grain boundaries. On the contrary, austenite grains grow remarkably at and above 1000 °C which in turn results in growth of martensite laths. This growth occurs due to the dissolution of the carbides at and above 1000 °C. It is evident from Fig. 1 that the volume fraction of carbides is higher for 7S and with the increase of temperature to 1000 °C, the dissolution of carbides occurred as shown in Fig. 1(b).

**Table 2** Details of heat treatment cycles employed in the study

| Designation | Heating cycle |
|---|---|
| 7S-solution treatment | 750 °C/0.5 h/air cooling (AC) |
| 10S-solution treatment | 1000 °C/0.5 h/AC |
| C-cryo treatment | −70 °C/2 h/AC |
| LA-low temperature aging | 250 °C/2 h/AC |
| A-peak aging | 500 °C/2 h/AC |

**Table 1** Chemical composition of the steel in wt%

| Element | C | Cr | Ni | Mo | Ti | S | P | Si | Mn | Al | N | Fe |
|---|---|---|---|---|---|---|---|---|---|---|---|---|
| % | 0.018 | 12.2 | 9.8 | 0.72 | 0.23 | 0.003 | 0.005 | 0.07 | 0.03 | 0.04 | 0.006 | Bal |

## Hardness

The hardness of steel at different aging temperature and time is plotted in Fig. 2. It can be seen that both isochronal and isothermal aging curves show a peak in hardness, after which the hardness decreased. This peak hardness may be caused by the formation of fine precipitates distributed uniformly throughout the matrix; the decrease in hardness after the peak is primarily due to over-aging, i.e., coarsening of the precipitates resulting in higher inter-precipitate spacing. At still higher temperatures, dissolution of the strengthening precipitates is responsible for the reduction in hardness.

The variation of hardness with aging temperature is shown in Fig. 2(a). The high hardness on aging in the temperature range of 450–500 °C may be due to the precipitation of nano-sized intermetallics in the martensite matrix. Hardness of the steel has increased by nearly 28% after aging at 500 °C for 1 h. Figure 2(b) shows the effect of aging time on the hardness of the steel at 500 °C. The hardness increased from 28 HRC in the solution-treated condition to 42 HRC after aging at 500 °C for 2 h, after which a drop in hardness was observed. A 33% increase in hardness was noticed after peak aging at 500 °C for 2 h.

## Tensile Strength

The variation in ultimate tensile strength (UTS) of the steel with each step of the heat treatment for both 7S and 10S conditions is illustrated in Fig. 3. It was observed that 10S showed higher UTS than that of 7S for all the conditions. The typical values obtained were in the range of 900–1,048 and 929–1,066 MPa for 7S and 10S, respectively. The average UTS of SC and SCLA were similar to that of the "S" samples for both solution treatment temperatures. Jaswin and Mohanlal [15] reported that no significant change was noticed in UTS for EN52 and 21-4N valve steel after cryogenic treatment and tempering/aging.

On the contrary, SCA showed a sharp increase in UTS for both 10S and 7S conditions. An increase of 14.7 and 16.4% in the UTS was observed for 10S and 7S samples, respectively, after peak aging. This increase in strength may be attributed to the formation of very fine intermetallic of Ni and Ti ($Ni_3Ti$) during aging treatment [1–4].

The variation in yield strength (YS) after heat treatment for both 10S and 7S samples is shown in Fig. 4. The difference in the YS between 7S and 10S conditions after S, SCLA, and SCA treatments was observed to be minimal, at less than 20 MPa. However, after the cryogenic treatment, the difference in YS for 7S and 10S samples was 40 MPa, with 10S showing a higher value. The YS has increased by 109 and 62 MPa for 10S and 7S samples, respectively, after cryogenic treatment. The increase in YS after the cryogenic treatment may be attributed to the transformation of retained austenite to martensite at cryogenic temperatures. This steel exhibits a $M_s$ (martensite start) temperature considerably below the room temperature and hence, complete transformation will occur only after the cryogenic treatment at −70 to −80 °C. The difference in YS for 7S and 10S after cryogenic treatment is primarily due to the difference in solution treatment temperature. For higher solution treatment temperature, there is more retained austenite and more carbide dissolution in the matrix. The carbide dissolution for 10S sample can be clearly seen in Fig. 1(b) with very few carbide particles. As the carbon content increases, the $M_s$ temperature of the steel decreases, retaining the higher amount of austenite during quenching [13, 14]. This also results in harder martensite after transformation of retained austenite by cryogenic treatment. On the contrary, a lower solution treatment

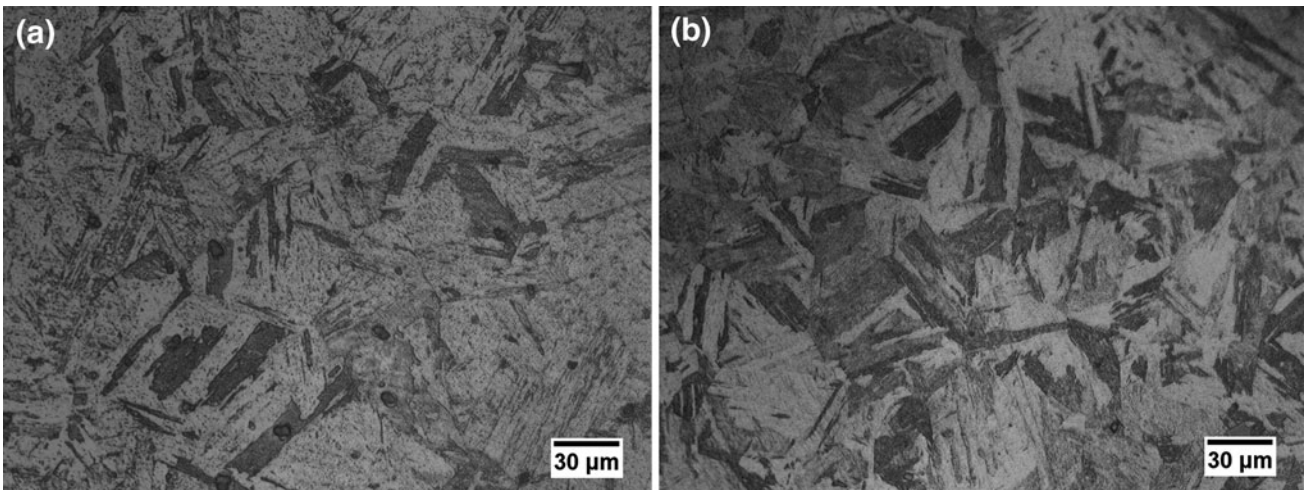


**Fig. 1** Microstructure of the 12Cr–10Ni–0.25Ti–0.7Mo steel after solution treatment at two temperatures (**a**) 750 °C, (**b**) 1000 °C

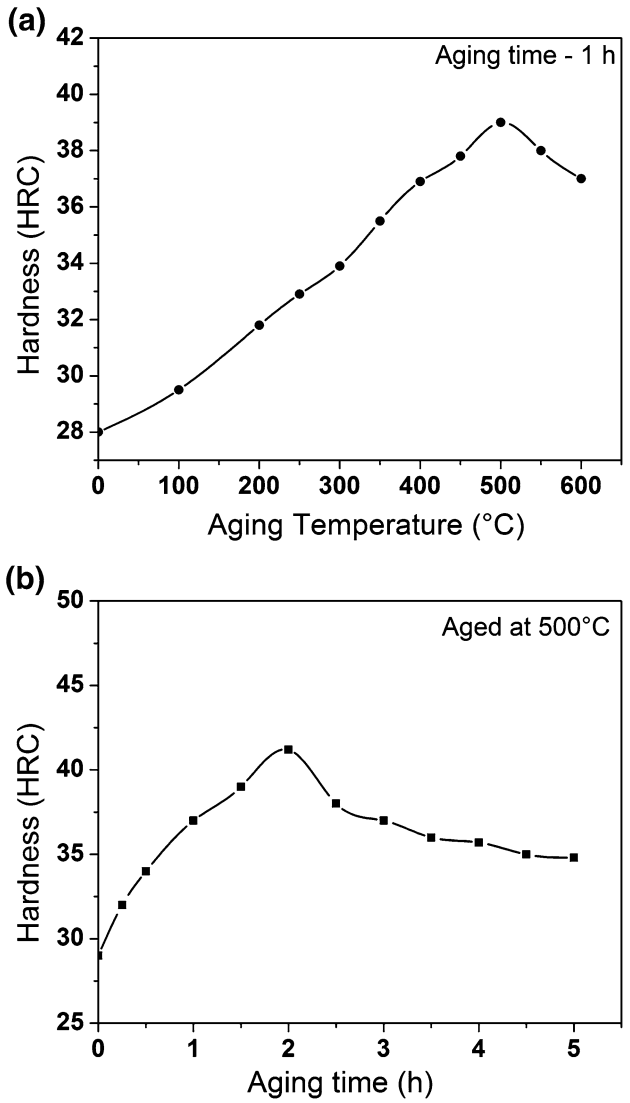


**Fig. 2** Effect of aging time and temperature on the hardness of 12Cr–10Ni–0.25Ti–0.7Mo steel (**a**) aging temperature, (**b**) aging time

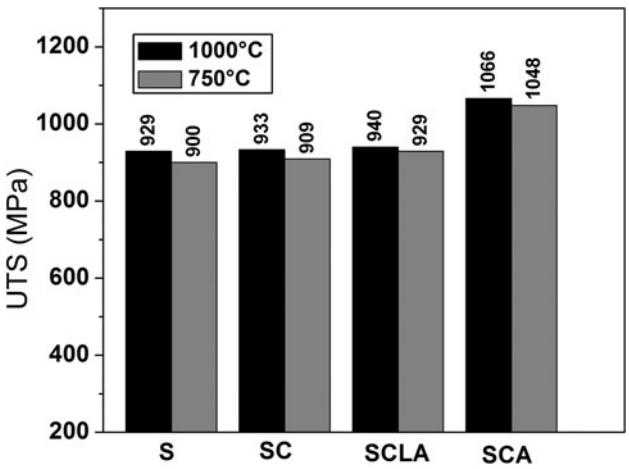


**Fig. 3** Effect of different heat treatment on the ultimate tensile strength of the 12Cr–10Ni–0.25Ti–0.7Mo steel

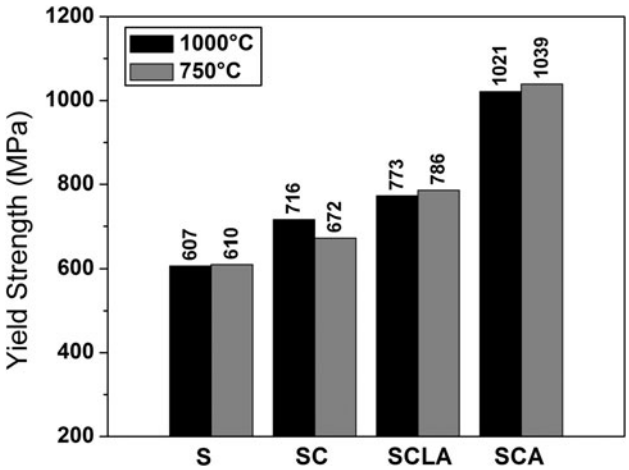


**Fig. 4** Effect of different heat treatment on the yield strength of the 12Cr–10Ni–0.25Ti–0.7Mo steel

temperature will result in a lower content of retained austenite with a higher volume fraction of carbides, as evident from Fig. 1(a). This lower content of retained austenite, which subsequently transforms to martensite, was responsible for the lower increase in YS after cryo treatment for solution-treated samples at 750 °C (62 MPa) compared to 10S (109 MPa) samples.

An increase of 166 and 186 MPa in YS was observed after low temperature aging for 7S and 10S conditions, respectively. This can be considered as an under aged condition, where precipitate nucleation begins and only few precipitates will grow in size, sufficient to strengthen the alloy. However, the peak strength is observed after aging at 500 °C where, an increase of 414 and 439 MPa in YS was observed for 7S and 10S conditions, respectively. This increase in YS is attributed to the formation of very fine $Ni_3Ti$ precipitates.

## Elongation

Figure 5 shows the variation in ductility of the steel after different heat treatment for a solution-treated sample at 750 and 1000 °C. The difference in the ductility of 7S and 10S was observed to be small for all the heat-treated conditions. After the sub-zero treatment, a ductility of 15.2 and 16.2% was observed for 10S and 7S conditions, respectively. A good ductility was retained after aging at 250 and 500 °C. This is quite interesting, considering the fact that good strength and ductility were obtained after aging. A ductility of 15.6 and 14.9% were observed for 10S and 7S conditions, respectively, after aging at 500 °C.

### Transmission Electron Microscopy (TEM)

The transmission electron micrographs of the solution-treated specimen are shown in Fig. 6. The bright-field (BF) image consists of typical lath martensite containing a high density of dislocations and retained austenite as shown in Fig. 6(a). The corresponding dark-field (DF) image is shown in Fig. 6(b) with retained austenite appearing bright. It can be seen that retained austenite is located between martensite lath. A blocky type of retained austenite is observed, as shown in Fig. 6(a, b). The selected area diffraction pattern (SAD) inserted in Fig. 6(a) shows the spot pattern corresponding to austenite (γ) and martensite (α).

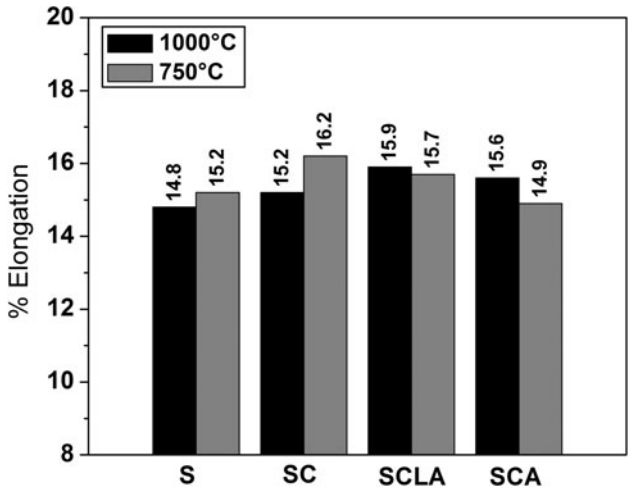


**Fig. 5** Effect of different heat treatment on the ductility of the 12Cr–10Ni–0.25Ti–0.7Mo steel

The BF micrograph of the solution-treated specimen, showing coarse, cube-shaped particles in the martensite matrix, is shown in Fig. 7(a). The EDS spectrum obtained from this particle is shown in Fig. 7(b). The spectrum shows the prominent peaks of Ti and N indicating that the particle is primarily Ti(C, N). The average size of the cube-shaped carbide in Fig. 7(a) was measured as 80–120 nm. The BF image, and corresponding EDS spectrum, of the irregularly shaped particle in the solution-treated sample is shown in Fig. 8(a and b), respectively. The BF image shows the irregularly shaped particle in addition to cube-shaped particle in martensite matrix. In Fe–C–Ni–Cr–Mo system, the carbide $M_{23}C_6$ occurs as $(Fe, Cr, Mo)_{23}C_6$ with an FCC crystal structure with a lattice parameter of 1.062 nm [17, 18]. The EDS spectrum obtained from the irregularly shaped particle shows prominent peaks of Cr, and Fe in addition to peaks of C and Mo. This spectrum indicates that the carbide is $M_{23}C_6$ type with chemical formula $(Fe, Cr, Mo)_{23}C_6$ as reported in literature [17].

The TEM micrographs of the steel aged at 500 °C for 2 h are shown in Fig. 9. The BF image of the sample with precipitate distribution in the matrix is shown in Fig. 9(a). The precipitates are very fine, with sizes in the range of 2–4 nm. The DF image of the precipitates and corresponding SAD pattern are shown in Fig. 9(b and c), respectively. The SAD pattern was analyzed to identify the

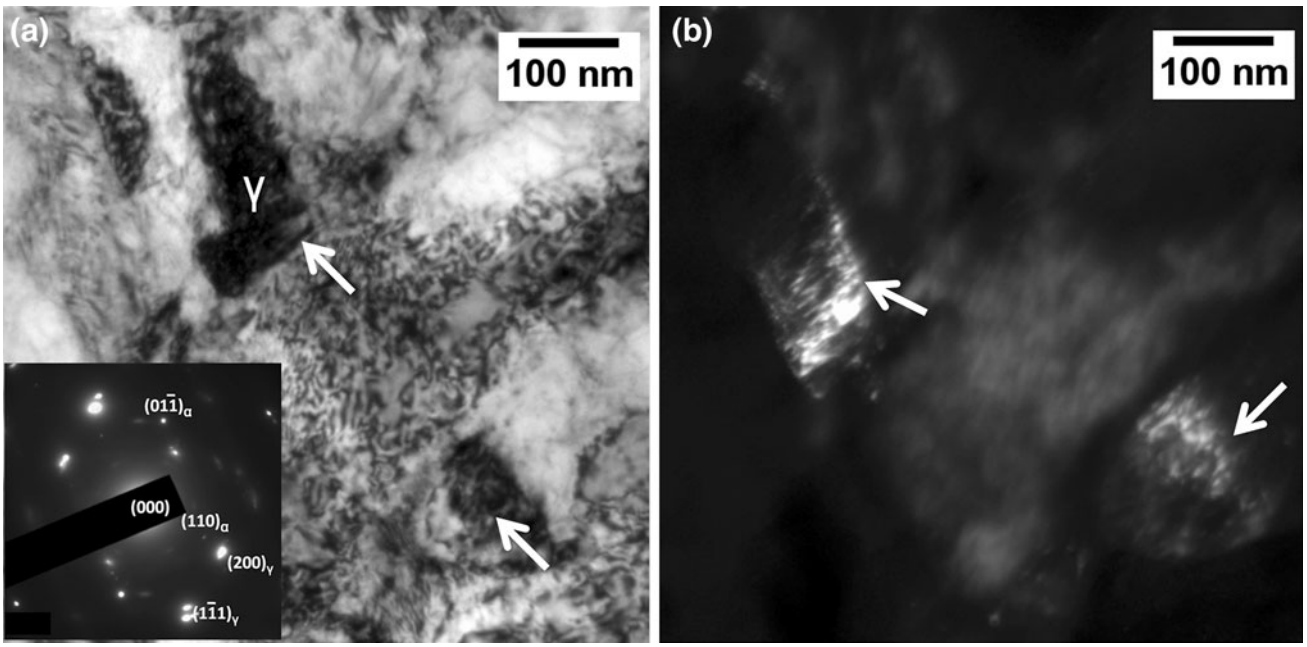


**Fig. 6** Transmission electron micrograph of the solution-treated specimen at 750 °C for 0.5 h followed by air cooling, martensite with retained austenite: (**a**) bright-field image of retained austenite and selected area diffraction pattern. (**b**) Dark-field image of retained austenite obtained using γ diffraction spot

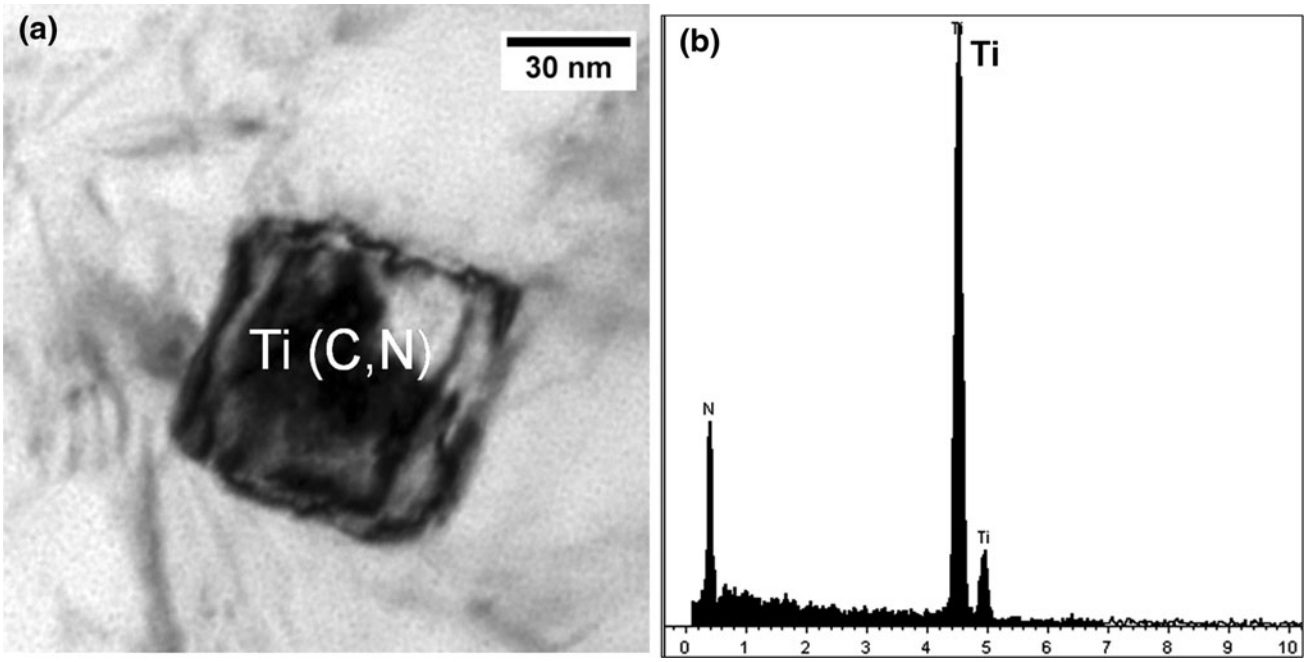


**Fig. 7** Transmission electron micrograph of the solution-treated specimen at 750 °C for 0.5 h followed by air cooling: (**a**) bright-field image of cube-shaped Ti(C, N) in martensite matrix. (**b**) EDS spectrum obtained from the Ti(C, N)

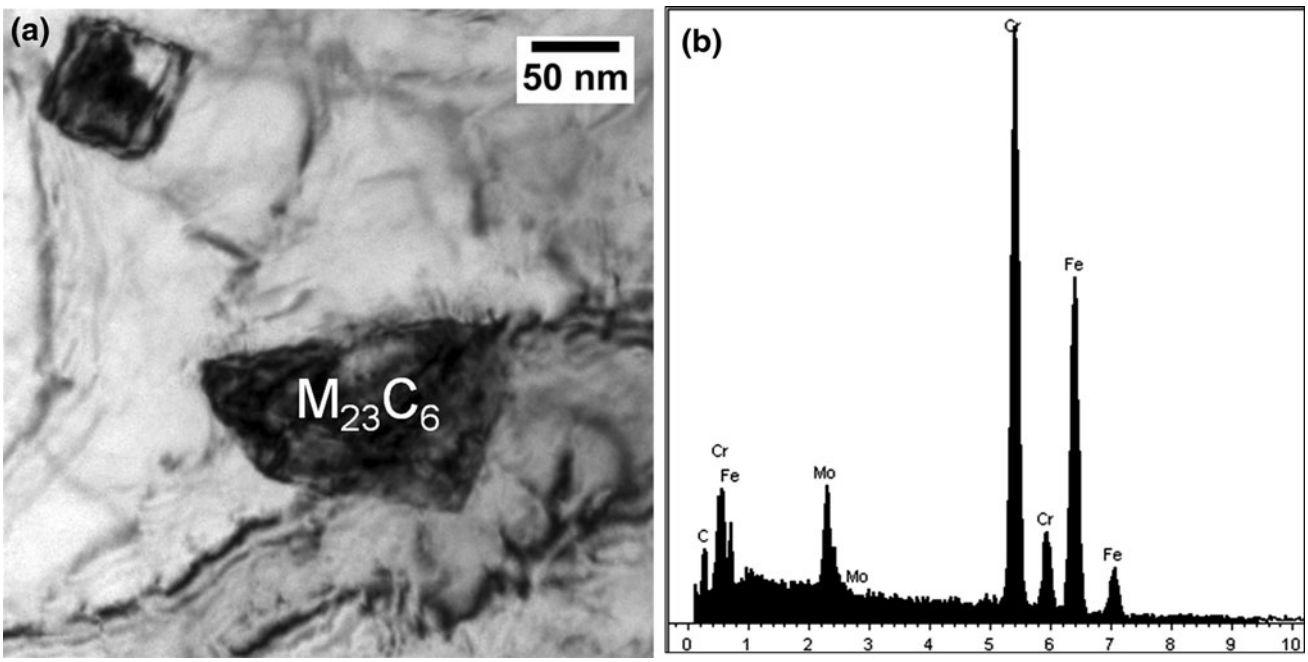


**Fig. 8** Transmission electron micrograph of the solution-treated specimen at 750 °C for 0.5 h followed by air cooling: (**a**) bright-field image of $M_{23}C_6$ carbide in martensite matrix. (**b**) EDS spectrum obtained from the $M_{23}C_6$ carbide

precipitate. As the diffraction patterns were quite complex, orientation relationships were used for interpretation, in addition to comparison with previous studies [1–4]. The pattern was indexed on the basis of the hexagonal η-$Ni_3Ti$ phase [3, 4]. The schematic of the SAD pattern with the spots indexed is shown in Fig. 9(d) and confirmed to be η-$Ni_3Ti$.

Compared to commercial, PH martensitic stainless steel, the present 12Cr–10Ni–0.25Ti–0.7Mo steel has lower precipitation hardenability which in turn results in lower

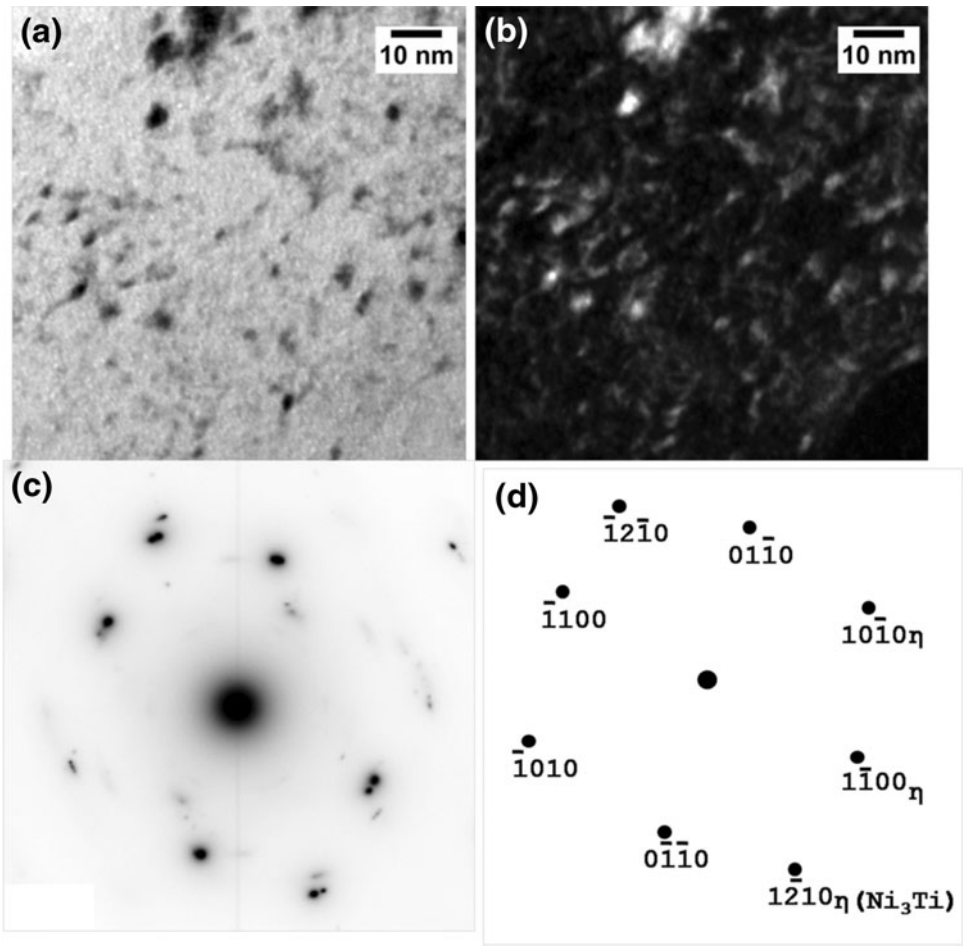


**Fig. 9** TEM image of the steel subjected to 7SCA treatment (**a**) bright-field image of the precipitates, (**b**) dark-field image of the precipitates, (**c**) selected area diffraction pattern, (**d**) schematic of SAD pattern

**Table 3** Increase in yield strength after aging, and precipitates responsible for strengthening in PH martensitic stainless steel [19–23]

| Material | Condition | % Increase in yield strength after peak aging | Precipitates |
|---|---|---|---|
| Present steel<br>12Cr–10Ni–0.7Mo–0.25Ti (wt%) | Solution treatment—1000 °C/0.5 h/AC<br>Aging—500 °C/2 h/AC | 68.85 | $Ni_3Ti$ |
| 17-4 PH<br>17Cr–4Cr–4Cu (wt%) | Solution treatment—1038 °C/0.5 h/AC<br>Aging—496 °C/4 h/AC | 34.5 | Cu |
| Custom 455<br>12Cr–9Ni–0.5Mo–1.4Ti–2Cu (wt%) | Solution treatment—843 °C/0.5 h/water quenching<br>Aging—510 °C/4 h/AC | 95 | Cu, $Ni_3Ti$ |
| 13-8 Mo PH<br>13Cr–8Ni–2.45Mo–1.3Al (wt%) | Solution treatment—830 °C/40 min/AC<br>Aging—482 °C/4 h/AC | 100 | NiAl |

tensile properties at room temperature. This is attributed to the fact that the present steel has a lower content of alloying elements participating in precipitation reaction. The typical alloying element content in commercial steels is typically on the order of a few weight percent: 17-4 PH (4 wt% Cu) [5, 6], 13-8 Mo PH (1.3 wt% Al) [19], Custom 455 (2.5 wt% Cu, 1.4 wt% Ti) [20]; in comparison, the steel in this study contained only 0.25 wt% titanium. The percentage increase in YS after aging and the precipitates responsible for age hardening in PH steels are shown in Table 3. An increase of 34.5, 100, and 95% in YS after aging was reported for 17-4 PH, 13-8 Mo PH, and Custom 455, respectively. On the other hand, the present steel showed an increase of 68.85% in YS. Among these four

steels, 13-8 Mo PH shows maximum increase in YS after aging, indicating that aluminum is a better precipitating element than Ti and Cu. It is interesting to note that the present steel and Custom 455 steel are strengthened by similar type of precipitates [20]. Nevertheless, Custom 455 steel gains its additional strength first, due to copper precipitates and second, due to the higher content of Ti.

## Conclusions

1. The microstructure of the solution-treated samples at 750 and 1000 °C consists of lath martensite, retained austenite, Ti (C, N), and $M_{23}C_6$ carbides. Retained austenite is seen between interlath films of martensite.
2. Age hardening started at a 250 °C and peak hardening occurred in the temperature range of 400–500 °C for holding time of 1–2 h due to formation of fine precipitates.
3. An increase of 27 and 68% in YS was observed on aging the solution-treated and cryogenic-treated samples at 250 and 500 °C, respectively.
4. The fine precipitates that form on aging are responsible for strengthening and the precipitates were identified as $\eta$-$Ni_3Ti$ precipitates.
5. A good combination of strength and ductility can be obtained by solution treatment at 1000 °C followed by cryogenic treatment and aging at 500 °C for 2 h.
6. Solution treatment temperatures (750 and 1000 °C) showed a minor effect on the mechanical properties of the studied steel.

**Acknowledgments** The authors would like to express their gratitude to the Director, VSSC for his kind permission to publish this study.

## References

1. A. Shekhter, H.I. Aaronson, M.K. Miller, S.P. Ringer, E.V. Pereloma, Effect of aging and deformation on the microstructure and properties of Fe–Ni–Ti maraging steel. Metall. Mater. Trans. A **35**(3), 973–983 (2004)
2. Y. He, K. Yang, W. Sha, Microstructure and mechanical properties of a 2000 MPa grade Co-free maraging steel. Metall. Mater. Trans. A **36**(9), 2273–2287 (2005)
3. U.K. Viswanathan, G.K. Dey, M.K. Asundi, Precipitation hardening in 350 grade maraging steel. Metall. Trans. A **24**(11), 2429–2442 (1993)
4. V.K. Vasudevan, S.J. Kim, C. Marvin Wayman, Precipitation reactions and strengthening behavior in 18 wt pct nickel maraging steels. Metall. Trans. A **21**(10), 2655–2668 (1990)
5. U.K. Viswanathan, S. Banerjee, R. Krishnan, Effects of aging on the microstructure of 17-4 PH stainless steel. Mater. Sci. Eng. A **104**, 181–189 (1988)
6. C.N. Hsiao, C.S. Chiou, J.R. Yang, Aging reactions in 17-4 PH stainless steel. Mater. Chem. Phys. **74**, 134–142 (2002)
7. H.J. Rack, D. Kalish, The strength, fracture toughness and low cycle fatigue behaviour of 17-4 PH stainless steel. Metall. Trans. **5**(7), 1595–1605 (1974)
8. F.B. Pickering, *Physical Metallurgy and the Design of Steels* (Applied Science Publishers, London, 1978)
9. X. Guang, X. Gan, G. Ma, F. Luo, H. Zou, The development of Ti-alloyed high strength microalloy steel. Mater. Des. **31**, 2891–2896 (2010)
10. Y. Han, J. Shi, L. Xu, W.Q. Cao, H. Dong, Effects of Ti addition and reheating quenching on grain refinement and mechanical properties in low carbon medium manganese martensitic steel. Mater. Des. **34**, 427–434 (2012)
11. A. Pardo, M.C. Merino, A.E. Coy, F. Viejo, M. Carboneras, R. Arrabal, Influence of Ti, C and N concentration on the intergranular corrosion behaviour of AISI 216Ti and 321 stainless steels. Acta Mater. **55**, 2239–2251 (2007)
12. H. Baker, H. Okamoto, *ASM Handbook, vol 03: Alloy Phase Diagrams* (ASM International, Materials Park, 1992)
13. C.H.I. Hong-xiao, M.A. Dang-shen, Y.O.N. Qi-long, W.U. Li-zhi, Zhang. Zan-pu, W. Yong-wei, Effect of cryogenic treatment on properties of Cr8-type cold work die steel. J. Iron. Steel Res. Int. **17**(6), 43–46 (2010)
14. M. El Mehtedi, P. Ricci, L. Drudi, S. El Mohtadi, M. Cabibbo, S. Spigarelli, Analysis of the effect of deep cryogenic treatment on the hardness and microstructure of X30 CrMoN 15 1 steel. Mater. Des. **33**, 136–144 (2012)
15. M.A. Jaswin, D. Mohanlal, Effect of cryogenic treatment on the tensile behavior of EN 52 and 21-4N valve steels at room and elevated temperatures. Mater. Des. **32**, 2429–2437 (2011)
16. S. Harish, A. Bensely, D. Mohanlal, A. Rajadurai, G.B. Lenkey, Microstructural study of cryogenically treated EN31 bearing steel. J. Mater. Process. Technol. **209**, 3351–3357 (2009)
17. Kh. Kuo, C.L. Jia, Crystallography of M23C6 and M6C precipitated in a low alloy steel. Acta Mater. **33**, 991–996 (1985)
18. D.W. Hetzner, W. Van Geertruyden, Crystallography and metallography of carbides in high alloy steels. Mater. Charact. **59**, 825–841 (2008)
19. D.H. Ping, M. Ohnuma, Y. Hirakawa, Y. Kadoya, K. Hono, Microstructural evolution in 13Cr–8Ni–2.5Mo–2Al martensitic precipitation-hardened stainless steel. Mater. Sci. Eng. A **394**(1), 285–295 (2005)
20. K. Stiller, M. Hättestrand, F. Danoix, Precipitation in 9Ni–12Cr–2Cu maraging steels. Acta Mater. **46**(17), 6063–6073 (1998)
21. A.K. Steel Corporation, 17-4 PH Stainless Steel Data Sheet, 17-4 PH-S-8-01-07
22. Carpenter Technology Corporation, Custom 455 Stainless Steel Technical Data Sheet (2006)
23. Y.S. Ding, L.W. Tsay, M.F. Chiang, C. Chen, Gaseous hydrogen embrittlement of PH 13-8 Mo steel. J. Nucl. Mater. **385**(3), 538–544 (2009)